Stabilization of Lattice Oxygen in Lithium Rich Cathode Materials via Manipulating Ni Content

Xiaoyuan Zhang[1,2,3]; Xiangnan Li[1,2,3]; Wenfeng Liu[1,2,3]; Huishuang Zhang[1,2,3]; Hongyun Yue[1,2,3]; Hongyu Dong[1,2,3]; Yongfang Li[4]; Shuting Yang*[1,2,3]; Yanhong Yin*[1,2,3]

[1]*School of Physics, School of Chemistry and Chemical Engineering, Henan Normal University, Xinxiang, Henan 453007,*

[2]*National and Local joint Engineering Laboratory of Motive Power and Key Materials, Xinxiang, Henan 453007, China*

[3]*Collaborative Innovation Center of Henan Province for Motive Power and Key Materials, Xinxiang, Henan 453007, China*

[4]*CAS Key Laboratory of Organic Solids, Beijing National Laboratory for Molecular Sciences, Institute of Chemistry, Chinese Academy of Sciences, Beijing 100190, China*

** Corresponding authors. E−mails addresses: shutingyang@foxmail.com*

Experimental Section

Material synthesis

$Li_{1.2}Ni_{0.2}Mn_{0.6}O_2$ (LR) and $Li_{1.13}Ni_{0.305}Mn_{0.565}O_2$ (HLR) were obtained via a solid-state reaction of Li_2CO_3 and precursor. The precursor was synthesized by a co-precipitation strategy, which has been reported in the early literature of our research group[1].

Characterization

X-ray powder diffraction (XRD) studies were performed with a Bruker Inc. (Germany) AXS D8 ADVANCE diffractometer in the range of 10-80° with a speed of 2°/min. Further structural analysis was carried out by the Rietveld structure refinement and the General Structure Analysis Software (GSAS, Los Alamos National Laboratory). The Raman spectroscopy information was collected by Raman spectrometer (Raman, LABRAM-HR) by argon-ion laser (λ = 532 nm). The X-ray photoelectron spectroscopy (XPS, GG314-JPS-9200) technique was used to characterize the chemical composition and valence state of the samples. The Electron paramagnetic resonance (EPR, BRUKER EMX-500 10/12) evaluations were

conducted at room temperature. High resolution transmission electron microscope (HRTEM, JEM-2100) with energy dispersive spectroscopy (EDS) mapping was carried out to detect the microstructures. Field emission Scanning electron microscopy (FESEM, HITACHI, SU8010) were performed to investigate the morphology of the samples. HAADF images were obtained with a cold field-emission gun and double-hexapole Cs correctors (CEOS GmbH, Heidelberg, Germany) and a scanning transmission electron microscope (JEOL, Tokyo, Japan) operated at 200 kV.

Galvanostatic charge-discharge experiments were carried out by CT2001A, Wuhan LAND Cell test system. The batteries were cycled at 0.1 C rate for the first three cycles and then cycled at 0.5 C rate. The galvanostatic intermittent titration (GITT) of the assembled cells was performed using a LAND-CT2001A battery test system between 2.1 and 4.8 V at room temperatures.

In-situ XRD observation:

In-situ XRD test was carried out to investigate the structural change of LR and LR-2 Li-rich materials during the charge and discharge processes. A detailed description of in-situ XRD cell for the Li-ion battery was employed. In detail, a thin aluminum window (thickness, 12μm) has been fixed on the cathode case of the cell as a sight window. The cathode was assembled at the bottom of the cell with the active material face upward. 45 μL of electrolyte 1 mol/L LiPF6 in ethylene carbonate/diethyl carbonate (EC/DEC) was homogeneously dropped onto the glassy fiber filter separator (GF/A, Whatman). The current and potential outputs from the potentiostat were recorded by a multifunction data acquisition module/amplifier (PGSTAT30 Differential Electrometer, Autolab), which was controlled by General Purpose Electrochemical Software (GPES). Typically, the galvanostatic control was carried out at a current density of 20 mA/g for initial cycle and the second charge process.

Electrochemical measurements

Slurries of positive electrodes composed of 80 wt % active material, 10 wt % super P carbon as conductive agent, and 10 wt % polyvinylidene fluoride (PVDF) as binder dispersed in N-methyl-2-pyrrolidene (NMP). The electrodes were prepared by spread the slurries onto aluminum foil, heated at 120 °C for 12 h in the vacuum oven. The

coated Al foils were then cut into circular electrodes of 12 mm diameter. In brief, coin-type cells 2025 (assembled in an argon-filled dry glovebox) were used to tested the electrochemical performance. Li-metal foils were used as the counter and reference electrodes. The nonaqueous electrolyte is ethylene carbonate-dimethyl carbonate (ECDMC) (1:1)/1 M $LiPF_6$ solutions (battery grade). The galvanostatic charge-discharge cycling was performed in the potential range of 2.1-4.8 V at a 0.1C rate for the initial three cycles, followed by cycling in the potential range of 2.1-4.8 V vs Li/Li^+ at a 1C rate in the subsequent cycles.

In situ DEMS measurements

In situ DEMS analysis was carried out to detect the gases generated during the initial charge–discharge process. The DEMS cell was assembled in an Ar-filled glove box. In all, the electrolyte was 1 M $LiPF_6$ dissolved in a mixture of ethylene carbonate （EC)-ethyl methyl carbonate (EMC) (volume ratio 1:1), and the porous polyethylene film was used as a separator. Electrodes were prepared by casting a slurry with a composition of 80 wt. % active materials, 10 wt. % Super P and 10 wt. % PVDF on to an aluminium current-collector foil. And the typical loading of the active material was 7-8 $mg \cdot cm^{-2}$ on an Al foil. The DEMS measurement was started 2–3 h before the cell was operated to obtain a stable gas evolution background. The electrochemical measurements were carried out at 0.1C for charge and discharge with a time interval of 50 ms between each DEMS sequence.

First-principles calculations

We have employed the Vienna Ab initio Simulation Package (VASP) to perform all density functional theory (DFT) calculations. The elemental core and valence electrons were represented by the projector augmented wave (PAW) method and plane-wave basis functions with a cutoff energy of 500 eV. Generalized gradient approximation with the Perdew-Burke-Ernzerh of (GGA-PBE) exchange-correlation functional was employed in all the calculations. Geometry optimizations were performed with the force convergency smaller than 0.01 eV/Å. The DFT+U approach was introduced to treat the highly localized Co and Ni 3d states ,using parameters of U–J = 3.9 and 6.2 eV, respectively. After geometry optimization, the projected density of

state (PDOS) plots were calculated. Spin-polarization effect was also considered. All the atom are relaxed in all the calculation. Supercells of $Li_{29}Mn_{15}Ni_4O_{48}$, $Li_{28}Mn_{14}Ni_6O_{48}$ were selected to represent $Li_{1.2}Mn_{0.6}Ni_{0.2}O_2$ and $Li_{1.13}Mn_{0.565}Ni_{0.305}O_2$, respectively.

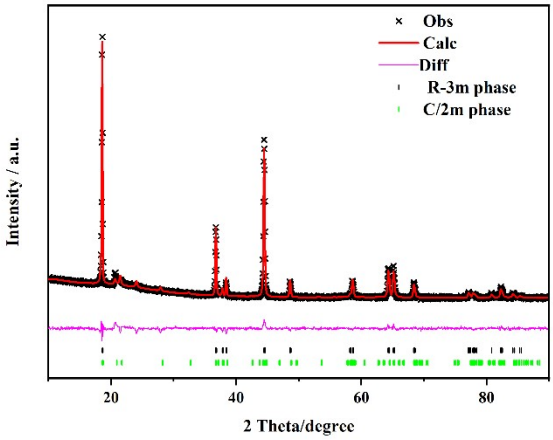

Fig. S1 Rietveld refinement patterns of the LR sample.

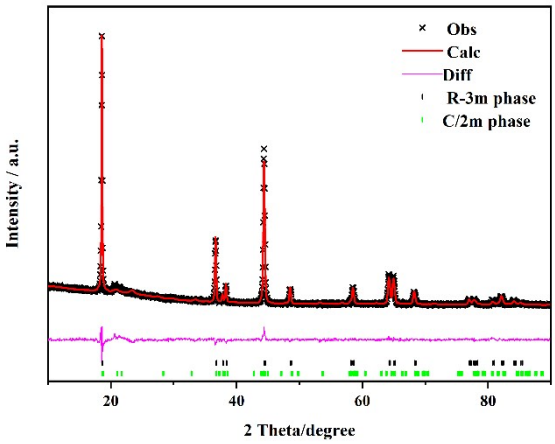

Fig. S2 Rietveld refinement patterns of the HLR sample

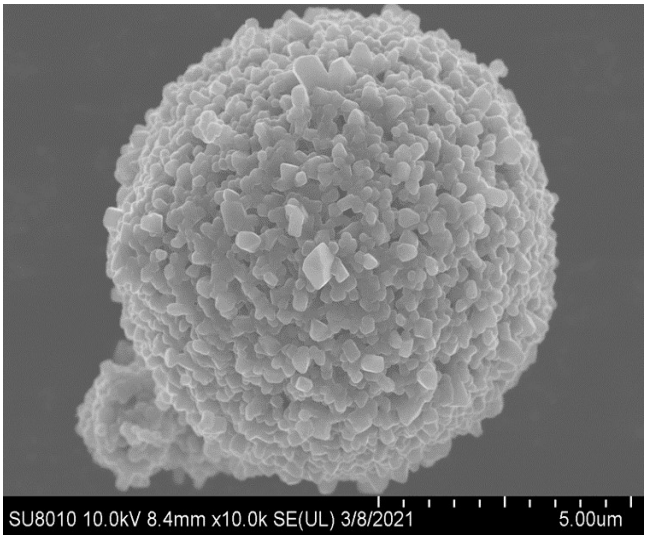

Fig. S3 Typical SEM images of LR

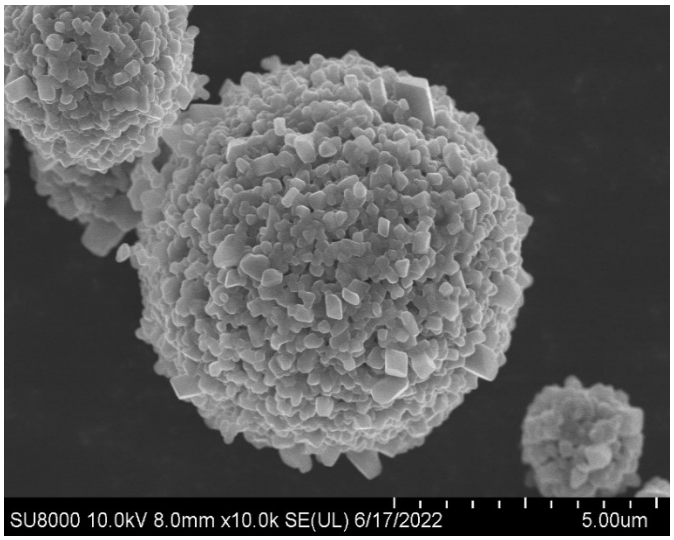

Fig. S4 Typical SEM images of HLR

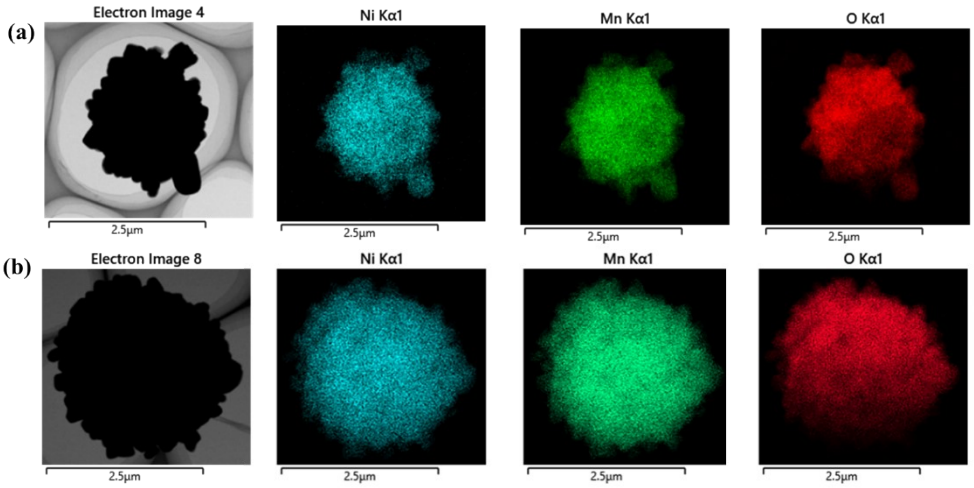

Fig. S5 The element mapping of the (a)LR and (b)HLR

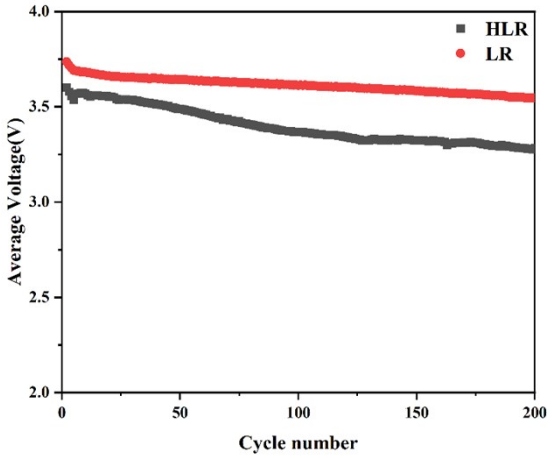

Figure S6. The plot of average voltage versus cycle number for LR and HLR during 200 cycles at 1.0 C at room temperature.

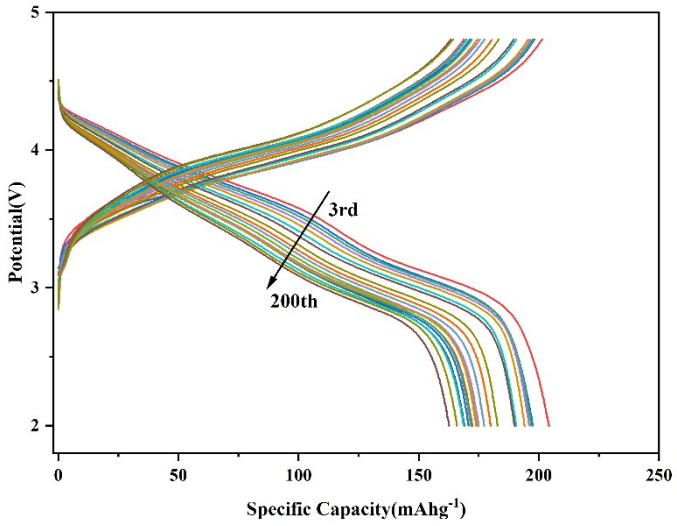

Fig. S7 Charge and discharge curves of LR within potential range of 2.1−4.8 V in 200 cycles.

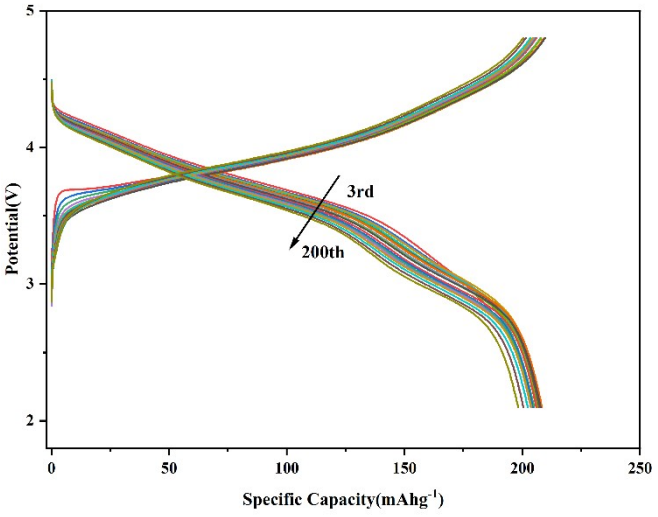

Fig. S8 Charge and discharge curves of LR within potential range of 2.1−4.8 V in 200 cycles

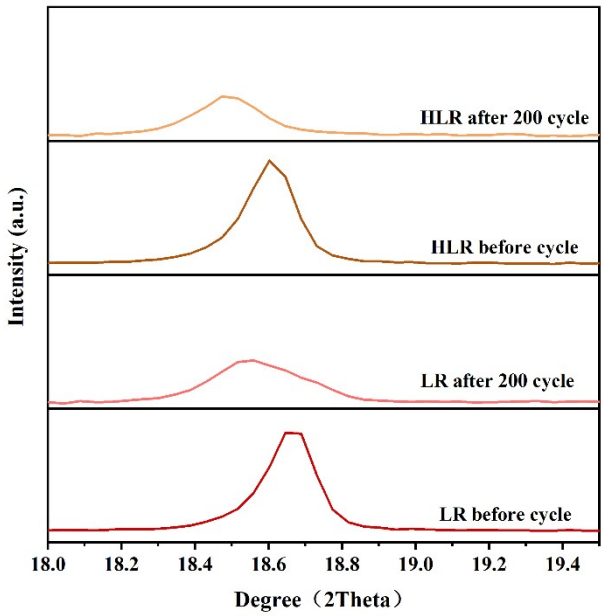

Fig. S9 The magnified XRD pattern of the (003) peak

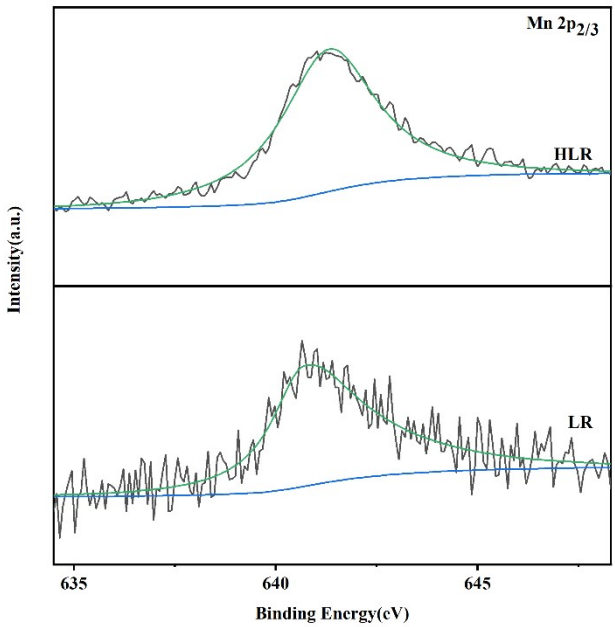

Fig. S10 High-resolution XPS spectra of Mn $2P_{3/2}$ in the fully discharged state after 200 cycles at the rate of 0.5 C

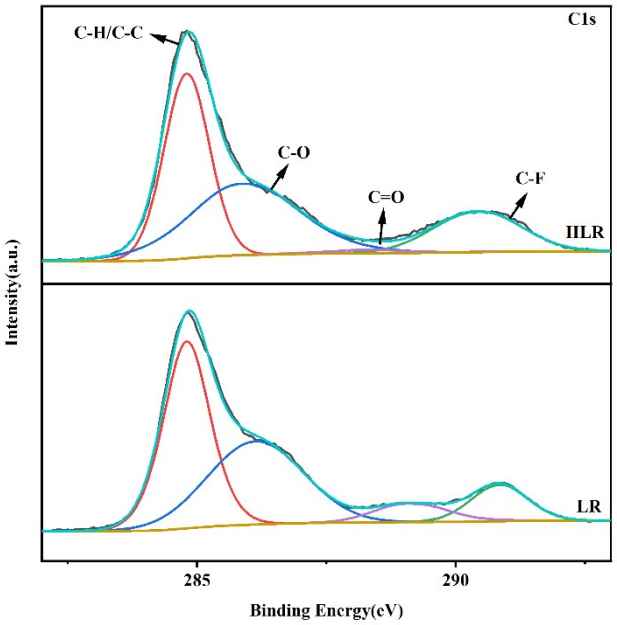

Fig. S11 High-resolution XPS spectra of C1s in the fully discharged state after 200 cycles at the rate of 0.5 C

Table S1 Detailed data obtained from Rietveld refinement of all samples

	R-3m(wt%)	C/2m(wt%)	Li/Ni	a/Å	c/Å	O occupancy
LR	65.5	34.5	3.99	2.863811	14.256989	0.9238
HLR	76.8	23.2	5.12	2.87058	14.301359	0.9578

Supplementary Note 1

The lithium ion diffusion coefficient is an important parameter influencing the rate performance of LIB electrode materials. Therefore, the GITT method was used to determine the lithium ion diffusion coefficient of LR and HLR sample. Fig. 3e-f shows the GITT curves during the first charge/discharge and the comparison of lithium ion diffusion coefficients of the two samples, respectively. The value of D_{Li^+} can be calculated by the following formula:

$$D_{Li^+} = \frac{4}{\pi\tau}\left(\frac{m_B V_m}{M_B S}\right)^2\left(\frac{\Delta E_S}{\Delta E_\tau}\right)$$

Where τ is 20 min, ΔE_s and ΔE_τ are obtained from charge-discharge voltage profiles,

while m_B is the loading amount of the active substance (g), M_B is the molecular weight of the material (g mol^{-1}), S is the surface area of the electrode (cm^2), and V_m is the molar volume of the material deduced from the crystallographic data (cm^3 mol^{-1}).

[1] X. Li, Z. Cao, H. Yue, Q. Wang, H. Zhang, S.-T. Yang, Tuning Primary Particle Growth of Li1.2Ni0.2Mn0.6O2 by Nd-Modification for Improving the Electrochemical Performance of Lithium Ion Batteries, Acs Sustain Chem Eng 7(6) (2019) 5946-5952.